PULSING AND CIRCULATION IN RIP CURRENT SYSTEM

D.P CALLAGHAN, T.E. BALDOCK, P. NIELSEN
[1]*Department of Civil Engineering, The University of Queensland, Brisbane 4072, Australia*

D.M. HANES[2], K. HAAS[3], J.H. MACMAHAN[4]
[2]*USGS Pacific Science Center, 400 Natural Bridges Drive, Santa Cruz, CA 95064*
[3]*Georgia Tech Regional Engineering Program, Savannah, GA, USA*
[4]*Oceanography Dept., Naval Postgraduate School, Monterey, CA 93940*

Current pulsations from a longshore bar and trough rip system located on the eastern coast of Moreton Island, Australia are presented. These pulsations occur over 10-20minute intervals through the rip system and are correlated to both water level gradients and wave energy variations. The field measurements suggest that rip current pulsations can be driven by fluctuating mass transport over the shore parallel inner bar.

1. Introduction

Rip currents occur in numerous locations along many sandy coastlines throughout the world and play an important role in cross-shore morphology *(Aagaard et al., 1997)*, have impacts on beach safety *(Short and Hogan, 1994)* and exists in many forms from topographic rips to transient rips *(Johnson and Pattiaratchi, 2004)*. The well recognised forcing mechanism for rip current circulation is the longshore variations in wave radiation stress gradient, i.e., setup and longshore currents *(Haas et al., 2002; Haller et al., 2002)*. In order to further understand this and other forcing mechanisms, particularly rip current pulsations and circulation patterns, an extensive field experiment was undertaken which included measurements of mean water levels, current velocities, bathymetry and circulation patterns. The data showed that pulsations in the shore-normal rip current velocities occur over 10-20 minute intervals and these are well correlated with fluctuating water level gradients (WLG) and current velocities in the shore parallel feeder currents. This implies that the rip pulsations are driven by a fluctuating mass transport over the shore parallel inner bar or fluctuations in longshore current, rather than standing long waves within the rip itself *(MacMahan et al., 2003)*. This is consistent with observed slow fluctuations in the wave energy further offshore.

2. Field Experiment

The field experiment was carried out on the eastern coast of Moreton Island during early February 2003 for three days. Moreton Island is a sand barrier island east of Brisbane and exposed to Pacific Ocean wave conditions as illustrated by Figure 1. The bathymetry conformed to the classic rip-feeder system, with two feeder channels inshore of an inner bar converging to a rip channel (Figure 2 and Figure 3). Figure 2 shows that the rip bathymetry has reasonably different northern and southern feeder channel and inner bar shapes. The rip neck channel also propagated north during the field work. However, the morphological state remained constant as a longshore bar and trough (LBT) after Short *(1999)*. Mean water levels were obtained with 1 cm accuracy from longshore transects of stilling wells in the feeder channels and outer trough ("+"on Figure 2). These were also supplemented with wells in the rip neck. Current velocities were obtained for both cross-shore and longshore flows (through rip neck and in the feeder channels) using pitot-style current meters ("•"on Figure 2) in a staggered arrangement with the stilling wells similar to Nielsen *(1999)*. Instrument spacing varying from 8 to 15m, with 12 stilling wells and 8 current meters covering a spatial domain of approximately 150m longshore and 45m cross-shore. Instrument locations were varied each day to follow the rip neck longshore movement.

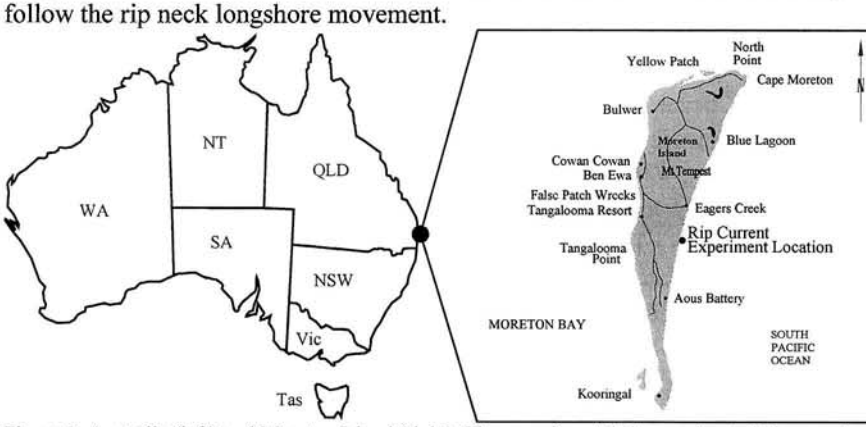

Figure 1. Australia (left) and Moreton Island (right). The experimental site was located 6km south of Eagers Creek.

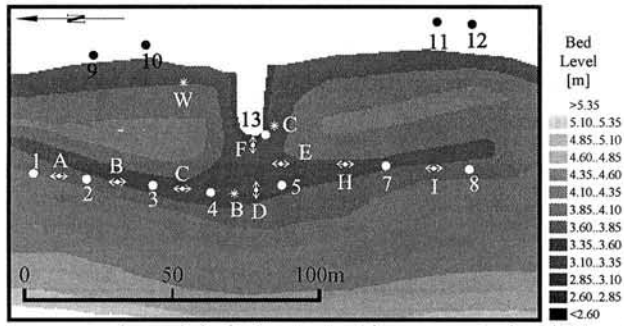

Figure 2. Rip current experimental site bathymetry and instruments (+ for stilling wells, • for pitot-style current meters and * for 'Aquadopp' current profilers) on Thursday 13 February 2003.

Three 'Aquadopp' current profilers ("*"on Figure 2) were also simultaneously deployed within the rip feeder (*B), rip neck (*C) and offshore of the inner bar (*W) to obtain both current and wave data. The experiment included video monitoring of dye releases from a bluff behind the field site. Bathymetry was obtained over a 300m by 180m region of the beach face and surf zone from total station and GPS surveys, out to a water depth of 2m. Offshore wave data was obtained from Brisbane wave buoy located 22km south and 16km east of the experimental site in 75m water depth. Figure 4 shows the experiment design, where a significant spatial proportion of the rip cell circulation was included for simultaneous measurements of WLG (from stilling wells), currents (from both pitot-style and Aquadopp current meters) and incident waves (pressure signal of *W measured at 1Hz).

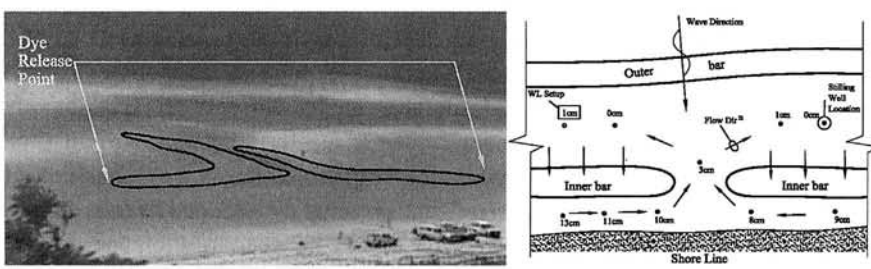

Figure 3. Left, 15 minute time averaged photo of the video monitoring of dye release. The dark region outlined illustrates the path of the dye, demonstrating the abrupt nature of rip current circulation. Right, flow patterns, mean water level setup and location of stilling wells for Wednesday Afternoon, 12th Feb 2003.

3. Measurements

Figure 2 shows the bathymetry and instruments deployed on 13 February 2003. This rip cell includes both northern and southern longshore feeder channels and a rip neck crossing perpendicularly through the inner bar (Figure 3(r)). Initial

monitoring using a 20minute sampling period during the falling tide of 12 February 2003 for approximately 4hours suggested the rip circulation incorporated a very long period pulsation with consistent hydraulic gradients as shown in Figure 3(r).

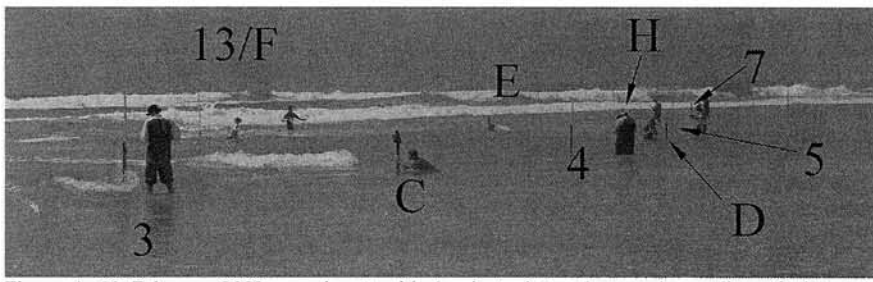

Figure 4. 13 February 2003 experiment with 1 minute interval manual sampling of pitot-style current meters and stilling wells.

Consequently, a decreased sampling period of one minute was adopted for an hour during Thursday morning monitoring which included stilling wells 3, 4, 5, 7 and 13 and pitot-style current meters C, D, H and F in parallel with video monitoring of dye releases. Figure 5 and Figure 6 shows the water level variations along with the hydraulic gradients which are generally towards the rip neck or offshore except for the southern feeder channel during the first eight minutes of measurements where the hydraulic gradient is very weakly away from the rip neck. The water level gradients for the southern feeder are a factor 5 less than those for the northern feeder and consequently produce a factor $\sqrt{5}$ less mass transfer. The current measurements on Thursday morning of longshore, v and cross-shore, u velocity from both the pitot-style and 'Aquadopp' current meters are illustrated on Figure 7 and Figure 8 and pulse at 10-15minute. Given the magnitude of the northern and southern feeder currents are qualitatively similar, it would appear the southern feeder is mostly longshore current (i.e., almost zero water level gradient) while the northern feeder is a combination of both longshore current (reducing effect) and rip setup circulations (aiding effect). However, the velocity measurements differ greatly between location and style of meter. For example, the cross-shore currents from the pitot-style meters are reasonably consistent except for between 11.1 and 11.3 hours in which the bar current strengthens while the near-shore current weakens. When comparing the pitot-style and 'Aquadopp' current meters for the northern feeder channel, we see no flow reversal from the pitot-style meters consistent with field observations (i.e., authors in the rip flow during measurements) yet significant flow reversal is recorded by the 'Aquadopp' current profile (height of water above instrument varied between 1.08 to 0.7m). However, Figure 9 shows the longshore velocities

measured by the two approaches pulse similarly in terms of signal shape. From testing, the pitot-style current meter acts analogous to a linear filter where the relation between actual and measured signals can be written as

$$\tau \frac{\partial m}{\partial t} + m = a, \tag{1}$$

where a and m are the actual and measured signals and τ is the filter time constant determined as 70s. This linear filter has the following response function, F_{LF}

$$F_{LF}(\omega) = (1 + i\omega\tau)^{-1}, \tag{2}$$

where $i = \sqrt{-1}$ and ω is the angular frequency. Similarly, the moving average approach used on the 'Aquadopp' measurements has the response function, F_{MA} of

$$F_{LF}(\omega) = (1 + i\omega\tau)^{-1}, \tag{3}$$

where T_{MA} is the moving average length adopted at 300s. If the two instruments are measuring identical hydrodynamics in the cross-shore direction and accepting the 'Aquadopp' response function is $F_{Aquadopp} \equiv 1$, applying (1) and (3) to the 'Aquadopp' measurements should yield pitot-style current meter readings. Figure 10(bottom) clearly demonstrates this is not the case. Further, the response functions plotted on figure 10(top) clearly shows the pitot-style current meters damping impact on the actual signal is less than that of the moving average analysis. The poor comparison in the cross-shore direction is believed to be a combination of: holding the pitot-style meter calibration parameter, C constant for strongly oscillatory flows ($v_{pitot} = C\sqrt{2g\Delta H}$, where v_{pitot} is the velocity, g is gravitational acceleration and ΔH is the distance of displaced oil in the pitot-style current meter); sensor location differences spatially (horizontally and vertically); and instrument errors (both). Nevertheless, the oscillations of cross-shore currents from both current meter styles pulse at similar periods albeit with different amplitudes. The balance of the analysis will isolate the two current meter styles to maintain consistency while recognising that comparable rip dynamics are inferred from both data sources.

Figure 11 shows that both the wave spectra offshore of the northern inner bar (*W on Figure 2) and in deep water (Point Lookout) are swell dominated with incident energy peaks near 14s. The shallow water energy peak occurs at T~250s (resolution of spectra is 0.002Hz). The time varying wave energy or "wave intensity", H_{rms}, was estimated using

$$H_{rms}(t,T) = 2\sqrt{2}\sqrt{\mathrm{var}\left\{\eta\left(t \in \left[t - \tfrac{T}{2}; t + \tfrac{T}{2}\right]\right)\right\}} \tag{4}$$

where H_{rms} is the root mean square wave height and T is the period over which

H_{rms} is estimated and was adopted in this analysis at five minutes. This H_{rms} signal exhibited tidal dependence (figure 12(top)) with significant red noise in its power spectrum (not shown) which are attributed to the non-removal of data trends *(Sonu, 1972)*. To clarify the pulsation period and to remove the red noise from the power spectrum, H_{rms} was quadratically detrended with the resulting spectrum (Figure 12(bottom)) inferring pulsations of periods ranging from 468s (7.8) to 851s (14.2 minutes). The very low frequency oscillation (around a period of 3125s) is presumably a by product of the quadratical detrending (i.e., not removing all the data trend) and not an unexplained physical fluctuation.

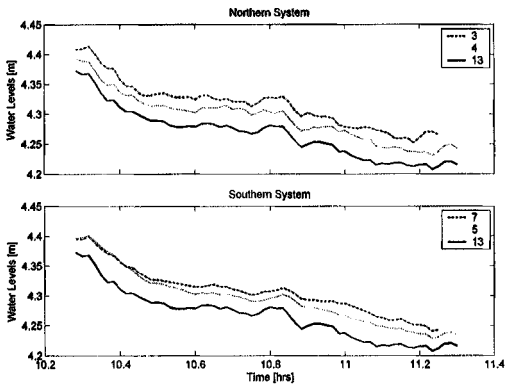

Figure 5. Five minute averaged water levels for the northern and southern systems obtained from the stilling wells on the 13 February 2003. Towards rip neck water level gradient occurs when 3>4>13 or 7>5>13.

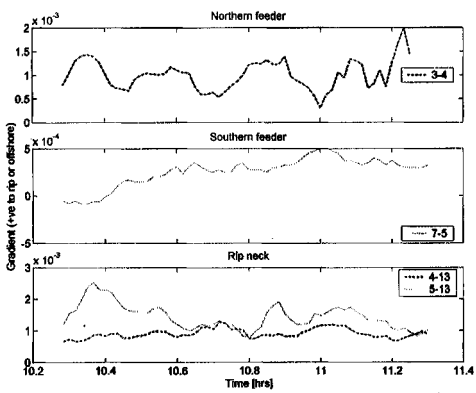

Figure 6. Five minute averaged water levels gradients for the northern and southern systems obtained from the stilling wells on the 13 February 2003.

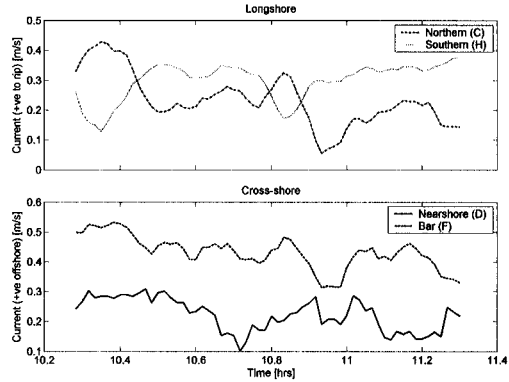

Figure 7. Five minute averaged longshore and cross-shore velocities on the 13 February 2003 obtained using the pitot-style current meters with positive flow in all panels indicating flow towards the rip neck or in an offshore direction.

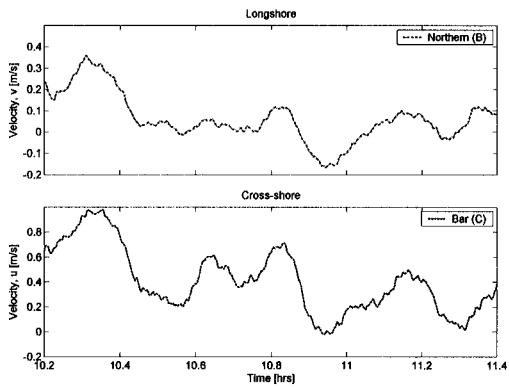

Figure 8. Five minute averaged longshore and cross-shore velocities on the 13 February 2003 obtained using the 'Aquadopp' current profilers with positive flow in all panels indicating flow towards the rip neck or in an offshore direction.

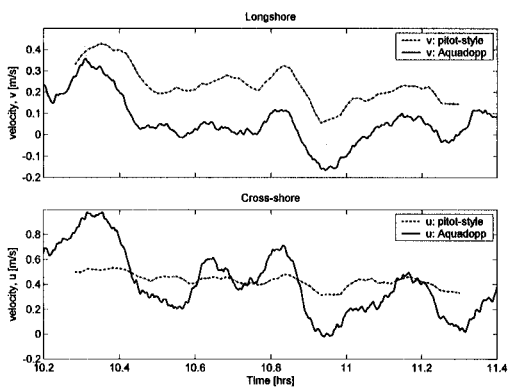

Figure 9. Five minute averaged northern longshore and cross-shore velocities obtained from the pitot-style current meters on the 13 February 2003.

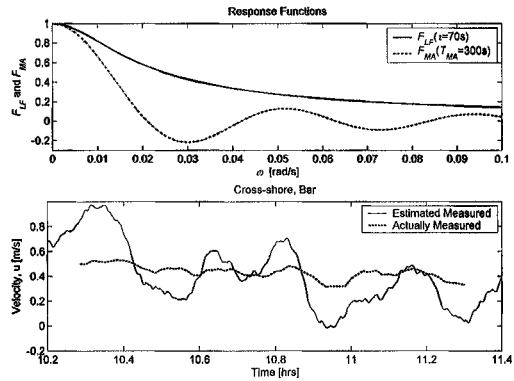

Figure 10. Top, response functions (2) and (3). Bottom, application of (1) and a five minute moving average to the 'Aquadopp' data (—, estimated measured) with the five minute averaged pitot-style current measurements (- - - -, actually measured).

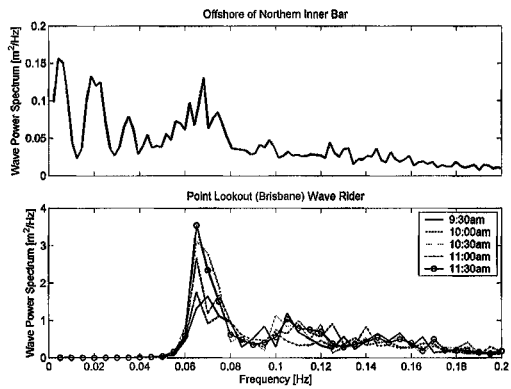

Figure 11. Top, wave spectra offshore of the northern inner bar (*W Figure 2). Bottom, deep water wave spectra (Point Lookout). All results are for the 13 February 2003.

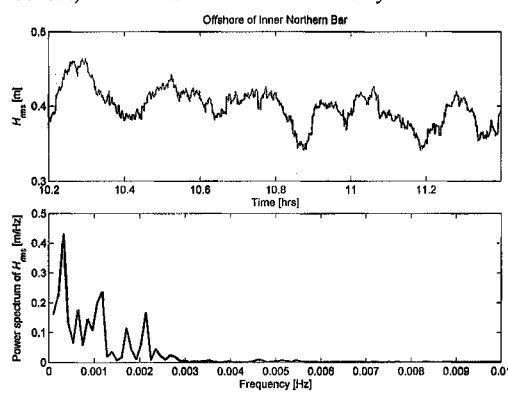

Figure 12. The wave intensity, H_{rms} offshore of the northern inner bar (top) and the power spectrum of H_{rms} (bottom). All results are for the 13 February 2003.

Similar to previous observations at Moreton Island *(Haas et al., 2002)*, the

rip circulation pattern (figures 1(r), 3 and 4) comprises two circular flow cells, with flow along the rip feeders converging and moving offshore via the rip neck. The flow then turned longshore offshore of the inner bar, and finally back over the inner bar, closing the circulation cell. The data indicate consistent WLG for all sections of the loop, except at the crossing of the inner bar, where water is pumped shoreward against the adverse gradient induced by wave setup. In particular, the stilling well data show forcing gradients away from the rip head in both longshore directions, consistent with the dye release observations (and a number of rip floats).

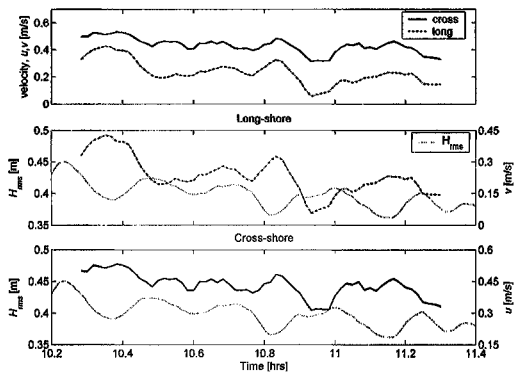

Figure 13. Northern feeder pitot-style current measurements compared with five minute wave intensity (H_{rms}) from offshore of the inner northern bar. All results for the 13 February 2003.

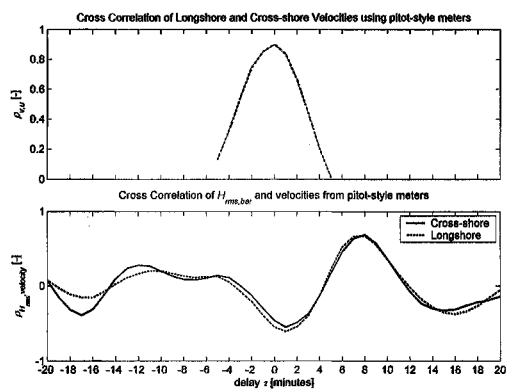

Figure 14. Northern feeder cross-correlations between longshore and cross-shore pitot-style velocities (top) and velocities individually with five minute H_{rms} (bottom). All results for the 13 February 2003.

The time series plot and cross-correlation between the northern longshore and cross-shore pitot-style currents and waves (Figure 13 and Figure 14) show that the velocity pulsations occur simultaneously with a period of 10-15 minutes and confirmed by the 'Aquadopp' current spectra (Figure 15 and Figure 16). However, the velocity pulsations strengthen while the H_{rms} pulsations weaken

(180° out of phase). As previously discussed, H_{rms} is fluctuating at between 8 and 15 minutes (Figure 11 & Figure 12). From Figure 7, it is seen that the southern feeder channel velocity is 180° out of phase with northern counterpart and the rip neck velocities. The weak hydraulic gradient in the southern feeder channel, while essentially towards the rip neck, does not exhibit pulsing but a general strengthening from 10.2 to 11 hours and then remaining approximately constant to 11.3 hours.

The in phase relationship between H_{rms} and the southern feeder indicates that this feeder dominates under high waves with water levels in the southern feeder elevated over the northern feeder (figure 5, wells 4&5) and during smaller H_{rms} conditions, the northern feeder strengthens. It is suggested that the gradient between well 5 to 4 indicates that the longshore current could block or limit the northern feeder currents through the rip neck (and thus pushing the northern feeder offshore directed current over the inner bar near the neck as observed) during high H_{rms}. This blocking effect reduces with falling H_{rms}, when the northern feeder flows through the rip neck channel.

Figure 17 & Figure 18 shows the five minute time-averaged longshore and cross-shore velocities and associated WLG for both feeder channels and the rip neck. The variations in the northern feeder current strength correlate well with WLG, with pulsations occurring over time-scales of 5-25minutes and again supporting the pump overpowering the longshore radiation stress gradient for decreasing waves. The southern feeder channel current, however, does not correlate well with WLG which supports the notion that these pulsations are the result of wide area pulsating longshore currents. The analogous cross-shore correlations are muddied as the mixing of feeder water is very limited (seen from the video monitoring of dye, Figure 3, where limited mixing occurred) and the current meters appear to be located in the northern feeder system. Similar time-scales are observed in wave height data from the wave measurements (Figure 12).

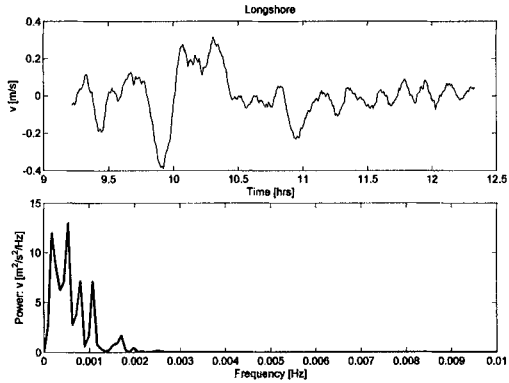

Figure 15. 13 February 2003 five minute averaged 'Aquadopp' currents (top panels) and spectra (bottom panels) for longshore (northern feeder) instrument.

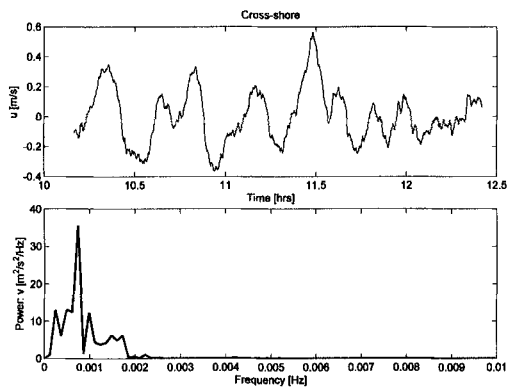

Figure 16. the 13 February 2003 five minute averaged 'Aquadopp' currents (top panels) and spectra (bottom panels) for cross-shore instruments.

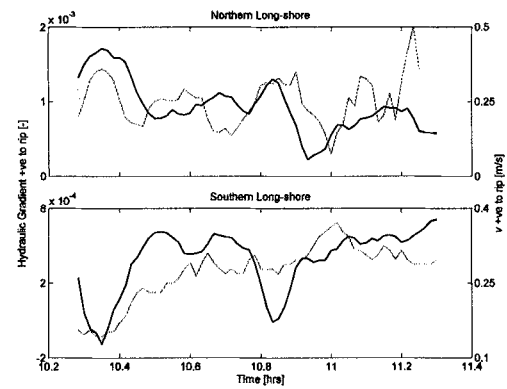

Figure 17. the 13 February 2003 five minute averaged longshore currents (—) and hydraulic gradients (- - -) from the pitot-style current meters and stilling wells respectively. Top and bottom panels separate out data from the northern and southern feeder channels respectively.

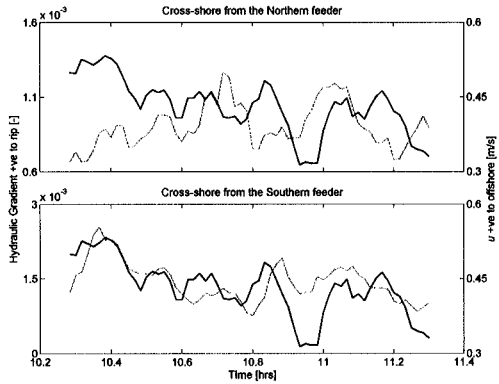

Figure 18. the 13 February 2003 five minute averagedcross-shore currents (—) and hydraulic gradients (- - -) from the pitot-style current meters and stilling wells respectively. Top and bottom panels separate out data from the northern and southern feeder channels respectively.

4. Conclusions

The model proposed by Aagaard et al *(1997)* for rip current speed relates the flow within the feeder channels and rip neck to mass transport over the inner bar, either through Stokes drift or wave rollers. The measured hydraulic gradients support this model and also suggest an additional mechanism for forcing rip current pulsations, which is very different from infragravity wave driven pulsations *(MacMahan et al., 2003)*. Assuming that the current velocities are related to the mass transport over the inner bar, then this will be a function primarily of wave height and period and channel cross-sectional area. Consequently, variations in the incoming wave height are likely to lead to similar variations in currents (or at least mass flow rate). This variation in incident wave height is usually considered for wave groups of period 1-4 minutes, but slower variations (5-20 minutes) in the incoming wave energy may also be present and the rip-feeder system is likely to respond more fully at these longer time-scales. This variation is not groups of groups, but a slow variation, in wave intensity.

The strong correlation between the northern longshore and cross-shore currents (Figure 14), in conjunction with the variations in wave intensity, suggests that Aagaard et al. *(1997)* simple mass transport balance or Nielsen et al. *(2001)* wave pumping models may provide a good description of rip pulsations with an appropriate phase delay for the waves, particularly pulses that occur at longer periods than those typically associated with wave groups. However, when combining the measurements from the southern feeder system, it appears the southern feeder was longshore current dominated and was responsible for introducing the phase different between the northern feeder channel current and H_{rms} pulsations.

Acknowledgments

The authors gratefully acknowledge support from the CRC Sustainable Tourism Project #52001, EPA Queensland and University of Queensland staff grants.

References

Aagaard, T., B. Greenwood and J. Nielsen, 1997. Mean currents and sediment transport in a rip channel. Marine Geology, 140, 25-45.

Haas, K.A., I.A. Svendsen, W. Brander Robert and P. Nielsen, 2002. Modelling of a rip current system on moreton island, Australia. Proceeding of the 28th International Conference on Coastal Engineering, World Scientific, Singapore, 784-796.

Haller, M.C., R.A. Dalrymple and I.A. Svendsen, 2002. Experimental study of nearshore dynamics on a barred beach with rip channels. Journal-of-Geophysical-Research, 107, 14-1 - 14-21.

Johnson, D. and C. Pattiaratchi, 2004. Transient rip currents and nearshore circulation on swell-dominated beach. Journal of Geophysical Research, 109, 1-20.

MacMahan, J.H., A.J.H.M. Reniers, E.B. Thornton and T.P. Stanton, 2003. Rip Current Pulsations on a Complex Beach. Journal of Geophysical Research, 109, 1-9.

Nielsen, P., 1999. Simple equipment for coastal engineering research and teaching. Proceedings Fifth International Conference on Coastal and Port Engineering in Developing Countries, 1029-1037.

Nielsen, P., R. Brander, W. and M. Hughes, 2001. Rip currents: Observations of hydraulic gradients, friction factors and wave pump efficiency. Proc Coastal Dynamics '01, ASCE, 483-492.

Nielsen, P., M. Hughes and R. Brander, W., 1999. A wave pump model for rip currents. Symposium on River, Coastal and Estuarine Morphodynamics, 415-423.

Short, A.D., 1999. Handbook of beach and shoreface morphodynamics. John Wiley, New York, xii, 379pp.

Short, A.D. and C.L. Hogan, 1994. Rip currents and beach hazards: their impact on public safety and implications for coastal management. Journal of Coastal Research, S.I., 197-209.

Sonu, C.J., 1972. Field observation of nearshore circulation and meandering currents. Journal-of-Geophysical-Research, 77, 3232-3247.